iPSC reprogramming of fibroblasts from a patient with a Rothmund-Thomson syndrome RTS

Vincent Gatinois, Romain Desprat, Lydiane Pichard, Fabienne Becker, Alice Goldenberg, Xavier Balguerie, Franck Pellestor, Jean-Marc Lemaitre

Stem Cell Research 45 (2020) 101807

Contents lists available at ScienceDirect

Stem Cell Research

journal homepage: www.elsevier.com/locate/scr

Lab resource: stem cell lines

iPSC reprogramming of fibroblasts from a patient with a Rothmund-Thomson syndrome RTS

Vincent Gatinois[a,b,d,#], Romain Desprat[a,c,#], Lydiane Pichard[a,b,c], Fabienne Becker[a,c], Alice Goldenberg[e], Xavier Balguerie[f], Franck Pellestor[a,b,d,2,*], Jean-Marc Lemaitre[a,c,1,*]

[a] IRMB, Univ Montpellier, INSERM, CHU Montpellier, Montpellier France
[b] Laboratory of Genome and Stem Cell Plasticity in Development and Aging, INSERM UMR1183, Montpellier, France
[c] SAFE-iPSC Facility INGESTEM, CHU de Montpellier, Montpellier, France
[d] Laboratory of Cytogenetics, ChromoStem Facility, Univ Montpellier, CHU de Montpellier, Montpellier, France
[e] Department of Medical genetics, CHU de Rouen, Univ Rouen, Inserm, Rouen U1079, France
[f] Department of Dermatology, CHU de Rouen, Rouen, France

A B S T R A C T

Rothmund-Thomson Syndrome (RTS) is a rare autosomal recessive disease that manifests several clinical features of accelerated aging. These findings include atrophic skin and pigment changes, alopecia, osteopenia, cataracts, and an increased incidence of cancer for patients. Mutations in *RECQL4* gene are responsible for cases of RTS. RECQL4 belongs to the RECQ DNA helicase family which has been shown to participate in many aspects of DNA metabolism. To be able to study the cellular defects related to the pathology, we derived an induced pluripotent cell line from RTS patient fibroblasts, with the ability to re-differentiate into the three embryonic germ layers.

Resource Table

Unique stem cell line identifier	*REGUi005-A*
Alternative name(s) of stem cell line	*RT iPSC*
Institution	*CHU Montpellier, Saint Eloi Hospital*
Contact information of distributor	Dr. Lemaitre: jean-marc.lemaitre@inserm.fr
Type of cell line	*iPSC*
Origin	*Human*
Additional origin info	*Age: 40* *Sex: Female* *Ethnicity: Caucasian*
Cell Source	*Fibroblast (skin biopsy)*
Clonality	*Mixed*
Method of reprogramming	*Sendaï*
Genetic Modification	*Yes*
Type of Modification	*Spontaneous mutation*
Associated disease	*Rothmund-Thompson syndrome*
Gene/locus	*RecQ like helicase 4/NM_004260.3 c.2269C>T*
Method of modification	*NA*
Name of transgene or resistance	*None*
Inducible/constitutive system	*None*
Date archived/stock date	*None*
Cell line repository/bank	*SAFE-iPS facility IRMB*
Ethical approval	*CPP CHU MONTPELLIER. 2014-A00178-39*

1. Resource utility

The DNA helicase RECQL4 is known for its roles in DNA replication and repair. RECQL4 mutations cause several genetic disorders including Rothmund-Thomson syndrome (RTS), characterized by developmental defects and predisposition to osteosarcoma (Lu et al., 2017). Here we reprogrammed fibroblasts with a homozygous *RECQL4* mutation (NM_004260.3 c.2269C>*T* hmz on the chromosome locus 8q24.3, Fig. 1, panel A) to induced pluripotent stem cells (iPSCs). These iPSCs are pluripotent and able to be differentiated into all three embryonic germ layers, providing a novel tool to further interrogate the role of RECQL4 DNA helicase in vitro. The resource we describe here will be useful in characterizing the role of RECQL4 in DNA damage repair and replication and provides a valuable tool for investigating how RECQL4 is involved in the premature aging pathologies.

2. Resource details

In this study, fibroblasts were obtained from a 40 years-old female with a diagnosed RTS. The patient displayed a small stature, scoliosis and a poikiloderma (characteristic RTS skin rash) on the face, lower limbs, buttocks and lower back. She had abnormal patella with bony

* Corresponding authors.
E-mail addresses: f-pellestor@chu-montpellier.fr (F. Pellestor), jean-marc.lemaitre@inserm.fr (J.-M. Lemaitre).
Authors contribute equally: Vincent Gatinois and Romain Desprat
1 Authors contribute equally: Franck Pellestor and Jean-Marc Lemaitre

https://doi.org/10.1016/j.scr.2020.101807
Received 8 December 2019; Received in revised form 21 March 2020; Accepted 25 March 2020
Available online 28 April 2020

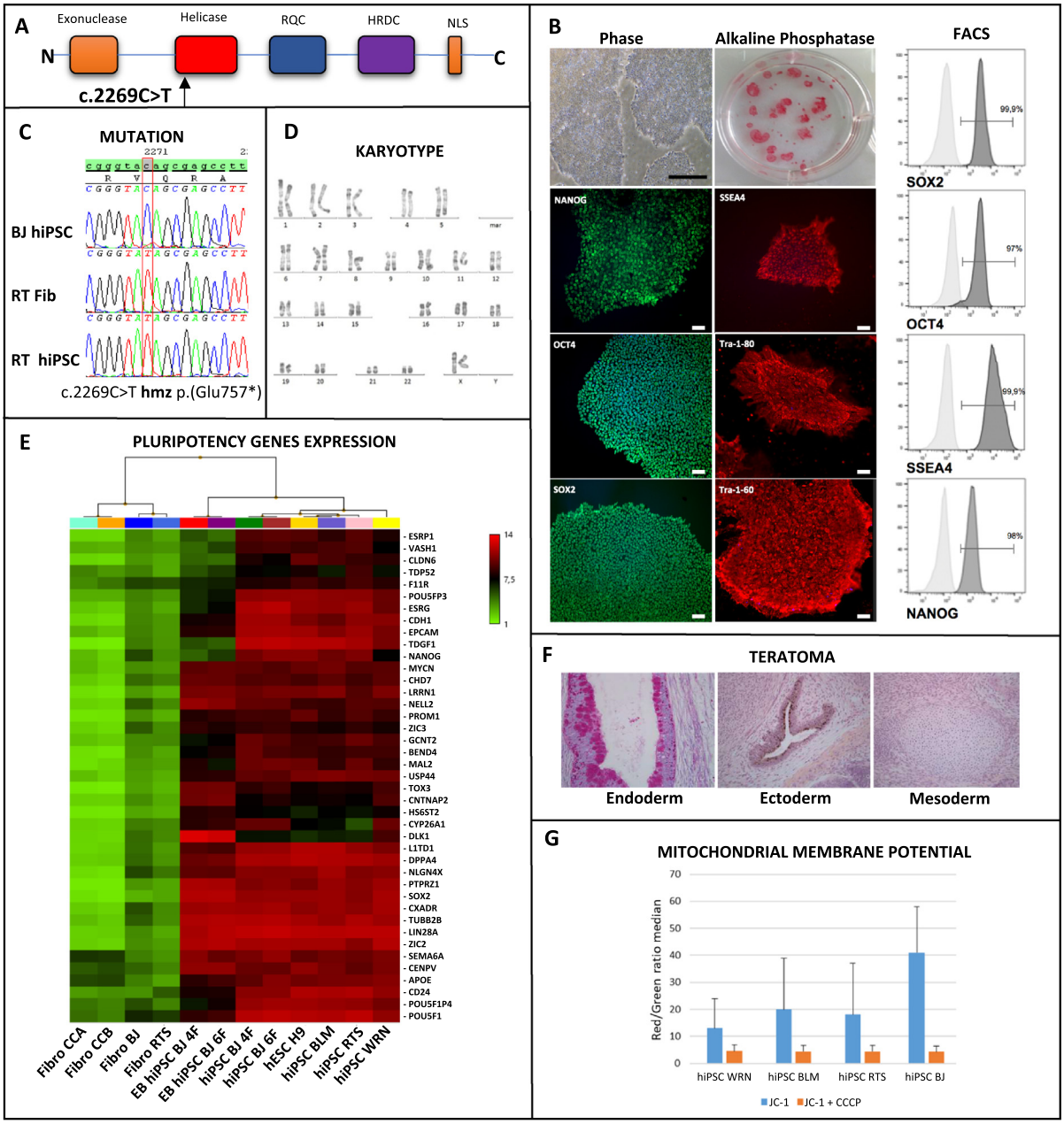

Fig. 1. RTS iPSC line characterization. 1A. Functional domains of the RECQL4 protein. Predicted locus of mutation is indicated with an arrow. 1B. RTS iPSC line pluripotency characterization: morphology on light microscopy (phase), alkaline phosphatase essay, pluripotency markers expression revealed by immunocytochemistry staining on fluorescent microscopy (NANOG, OCT4, SOX2, SSEA4, Tra-1-80 and Tra-1-60, scale bar: 50 μm) and FACS analysis (SOX2, OCT4, SSEA4, and NANOG). 1C. RTS mutation locus sequenced by standard Sanger method in a control (BJ hiPSC), the parent cell line (RT Fib), and the RTS iPSC line (RT hiPSC). 1D. R-banding karyotyping of RTS iPSC line. 1E. Supervised clustered heatmap of pluripotency gene expression. The colored scale from green to red shows the overexpression factor in comparison with the B2M housekeeping gene expression. 1F. Teratoma formation in immune-compromised mice. Histological sections stained with Hematoxylin-Eosin-Saffron. 1G. Mitochondrial membrane potential was measured by flow cytometry with JC-1 dye alone (blue boxes) or JC1-dye and CCCP as a negative control (orange boxes). Values are green (529 nm)/red (590 nm) ratios fluorescence intensity.

outgrowths. We generated the Cell line with the four reprogramming factors OCT3/4, SOX2, KLF4, and c-MYC transiently expressed in fibroblasts using the integration-free Sendai virus gene-delivery method. RTS iPSC cell line had normal morphology (Fig. 1, panel B, bright field microscopy, scale bar: 50 μm) and a normal diploid female karyotype 46,XX (Fig. 1, panel D). After about 10 passages, the expression of pluripotency markers was evidenced by flow cytometry staining, using antibodies against human OCT4, SSEA4, SOX2 and NANOG (Fig. 1, panel B) and by immunocytochemistry using the cell surface markers NANOG, OCT4, TRA-1–60, SOX2, NANOG, TRA-1–80 and SSEA4 (Fig. 1, panel B). Pluripotency was substantiated by the ability of RTS iPSC to differentiate into the three embryonic germ layers in vivo, as confirmed by the formation of teratoma in an immunosuppressed mouse. The histological study showed the presence of intestinal epithelium-derived structures (endoderm), neural tube-derived structures and melanocytes-like cells (ectoderm), and cartilage-derived structures (mesoderm) (Fig. 1, panel F). The expression of the pluripotency genes whose *OCT4, NANOG, SOX2* was assessed by transcriptomics: genes involved in pluripotency state (Guenther et al., 2010) were highly expressed and genes known to be expressed in fibroblast were down-regulated (Fig. 1, panel E, supervised heatmap of transcriptome analysis performed on fibroblasts from GEO Samples GSM1566208 (Fibro CCA

Table 1
Characterization and validation.

Classification	Test	Result	Data
Morphology	Photography	*Visual record of the line: normal colonies*	*Fig. 1 panel B*
Phenotype	Qualitative analysis (Immunofluorescence and Flow Cytometry)	*Oct4, Nanog, Sox2, Nanog, SSEA4, Tra–1–81, Tra–1–60*	*Fig. 1 panel B*
	Quantitative analysis (Flow Cytometry)	*Oct3/4:100%, Nanog: 100%, SSEA-4: 100%, SOX-2: 100%*	*Fig. 1 panel B*
Genotype	- Karyotype (G-banding)	*46XX (resolution 450)*	*Fig. 1 panel D*
	- CNV microarray	*No additional CNV*	*Suppl. material 1*
Identity	STR analysis	*DNA profiling*	*Not performed*
		18 STR were sites tested, and matched between the original cell lines and the reprogramed one	*Suppl. material 2*
Mutation analysis (IF APPLICABLE)	Sequencing	*NM_004260.3 c.2269C > T hmz*	*Fig. 1 panel C*
	Southern Blot or WGS	*Not performed*	*Not available*
Microbiology and virology	Mycoplasma	*Tested by luminescence, as Negative*	*Suppl. material 3*
Differentiation potential	Teratoma formation	*Detection of the presence of the three embryo germ layer by histochemistry (validated by a certified Anatomo-Histopathologist)*	*Fig. 1 panel F*
Donor screening (OPTIONAL)	HIV 1 + 2 Hepatitis B, Hepatitis C	*Negative by Elisa analysis*	*Not shown but available with authors*
Genotype additional info (OPTIONAL)	Blood group genotyping	*Not performed*	Not available
	HLA tissue typing	*Not performed*	Not available

Table 2
Reagents details-RT iPSC.

Antibodies used for immunocytochemistry/flow-Cytometry			
	Antibody	**Dilution**	**Company Cat # and RRID**
Pluripotency Markers Immunostaining	*Oct-4A Rabbit mAb (Clone C30A3) IgG*	*1:200*	*Cell Signaling Technology Cat# 2840, RRID:AB_2167691*
Pluripotency Markers Immunostaining	*Sox2 XP® Rabbit mAb (Clone D6D9) IgG*	*1:200*	*Cell Signaling Technology Cat# 3579, RRID:AB_2195767*
Pluripotency Markers Immunostaining	*Nanog XP® Rabbit mAb (Clone D73G4) IgG*	*1:200*	*Cell Signaling Technology Cat# 4903, RRID:AB_10559205*
Pluripotency Markers Immunostaining	*SSEA4 Mouse mAb (Clone MC813) IgG3*	*1:200*	*Cell Signaling Technology Cat# 4755, RRID:AB_1264259*
Pluripotency Markers Immunostaining	*TRA–1–60(S) Mouse mAb (Clone TRA–1–60(S)) IgM*	*1:200*	*Cell Signaling Technology Cat# 4746, RRID:AB_2119059*
Pluripotency Markers Immunostaining	*TRA–1–81 Mouse mAb (Clone TRA–1–81) IgM*	*1:200*	*Cell Signaling Technology Cat# 4745, RRID:AB_2119060*
Pluripotency Markers Flow cytometry	*PE Mouse anti-human Nanog (Clone: N31-355)*	*1:5*	*BD Biosciences Cat# 560791, RRID:AB_1937305*
Pluripotency Markers Flow cytometry	*PerCP-CyTM 5.5 Mouse anti-Oct3/4 (Clone:40/Oct-3)*	*1:5*	*BD Biosciences Cat# 560794, RRID:AB_1937313*
Pluripotency Markers Flow cytometry	*Alexa FluorR 647 Mouse anti-Sox2 (Clone: 245610)*	*1:5*	*BD Biosciences Cat# 560301, RRID:AB_1645308*
Pluripotency Markers Flow cytometry	*Alexa FluorR 647 Mouse anti-SSEA-4 (Clone: MC813-70)*	*1:5*	*BD Biosciences Cat# 560796, RRID:AB_2033991*
Pluripotency Markers Flow cytometry	*PE Mouse IgG1, κ Isotype Control (Clone MOPC-21)*	*1:5*	*BD Biosciences Cat# 554121, RRID:AB_395252*
Pluripotency Markers Flow cytometry	*PerCP-Cy5.5 Mouse IgG1, κ Isotype Control (Clone: X40)*	*1:5*	*BD Biosciences Cat# 347202, RRID:AB_400265*
Pluripotency Markers Flow cytometry	*Alexa Fluor® 647 Mouse IgG2a, κ Isotype Control (Clone: MOPC-173)*	*1:5*	*BD Biosciences Cat# 558020, RRID:AB_396989*
Pluripotency Markers Immunostaining	*Secondary Antibody Alexa Fluor® 488 conjugate Goat anti-Rabbit IgG*	*1:400*	*Invitrogen-Thermo Fisher Scientific Cat# A-11034, RRID:AB_2576217*
Pluripotency Markers Immunostaining	*Secondary Antibody Alexa Fluor® 555 conjugate Goat anti-Rabbit IgG*	*1:400*	*Invitrogen-Thermo Fisher Scientific Cat# A-21424, RRID:AB_141780*
Primers			
	Target	**Forward/Reverse primer (5′ − 3′)**	
RT mutation (Sanger sequencing)	*RT mutation*	*5′CATGGTCCCATCCCACTGAC3′*	
		5′CTGCAGGAAGAGGTGGCAG3′	

and CCB), fibroblasts BJ (Fibro BJ), fibroblasts from the RTS patient (Fibro RTS), iPS derived from BJ fibroblasts with 4 reprogramming factors OSKM or 6 factors OSKMNL (Lapasset et al., 2011), respectively (hiPSC BJ 4F and hiPSC BJ 6F) and the corresponding Embryoids Bodies harvested at 15 days of differentiation (EB hiPSC 4F and EB hiPSC 6F), the human embryonic pluripotent stem cell line H9 (hESC H9) and 3 iPSCs obtained from RECQL helicases mutated Werner syndrome patient (hiPSC WRN) (Gatinois et al., 2019a), RTS patient (hiPSC RTS), and Bloom syndrome patient (hiPSC BLM) (Gatinois et al., 2019b) respectively). The common genetic identity of RTS iPS cell line and parental fibroblasts was confirmed by the presence of the disease-associated mutation in the *RECQL4* gene by DNA 5′-Sanger sequencing (Fig. 1, panel C, capital letters correspond to exonic nucleotides, lower case letters correspond to intronic nucleotides. Location of DNA sequences variations are mentioned with red boxes). Microsatellite analysis showed matching profiles of short tandem repeats (STR) amplified from a genomic DNA RTS hiPS cells and patient-derived fibroblasts (Supplementary material 2 - RTS hiPSC STR analysis). The cell line was also confirmed to be free of mycoplasma (Supplementary material 3 - RTS hiPSC mycoplasma test). Mitochondrial membrane potential of hiPS RTS line was measured, in parallel with hiPS WRN and hiPS BLM cell lines, with JC-1 staining and flow cytometry analysis showing a global decrease for all these RECQL helicase diseases in comparison with a normal hiPS BJ cell line (Fig. 1, panel G, JC-1 red/green fluorescent absorption rates in orange bars, negative control by adding a CCCP membrane-potential disruptor in blue bars).

3. Materials and methods

3.1. Purification of fibroblasts from a fibroblast punch

A 1 mm-punch skin biopsy in 1 mL fibroblast medium (DMEM, 10% FBS) was cut into 10–12 pieces with a scalpel and transferred in a T25 culture flask. The flask was incubated in hypoxic conditions (37 °C, 5% CO2, 5% O2) for 1 day. Two supplements of 1 mL and 3 mL medium culture were added on day 2 and day 4. Culture incubation was sustained as needed changing medium every 2–3 days.

3.2. Reprogramming fibroblasts into iPSCs

The day before transfection, plate 5 × 10^4 fibroblast cells in each well of a 12-well plate in fibroblast medium (DMEM, 10%FBS). Culture fibroblast cells in an incubator (37 °C, 5% CO2, 5% O2) overnight to make sure that cells extend and adhere to the dish. The cells were transduced by Sendai-virus using the CytoTuneR-iPS 2.0 Sendai Reprogramming Kit (Thermo Fisher Scientific, cat#A34546), delivered with a Multiple Of Infection (MOI) of 10–10–6 (KOS MOI = 10, hc-Myc MOI = 10, hKlf4 MOI = 6) without polybrene. Manual clones picking was performed and then combined in a unique iPSC population. Cell culture was maintained in the Essential 8™ (Gibco) medium on Matrigel®- coated dishes with a daily morphology follow-up. Since 80% confluence was achieved, iPSC passaging was performed with the Versene Solution® (Gibco) dissociation agent and seeded with a 1/5 split ratio

iPSC culture and genomic DNA extraction iPS cells were then maintained on extracellular matrix Matrigel (Fisher Scientific, no.354277) in Essential 8™ culture media (Thermo Fisher Scientific, no. A15169-01), according to the manufacturer's instruction at 37 °C in 5% O2 and 5% CO2. DNA extraction was performed using the QIAamp DNA Mini Kit (Qiagen), following the manufacturer's instructions.

3.3. Karyotyping

It was performed on actively dividing cells on RHG-banding (Fig. 1D), using standard procedures at the ChromoStem® facility (Montpellier, France, http://www.chumontpellierfr/fr/chercheurs/plateformes/les-plateformesrecherche/chromostem/). A minimum of 10 to 15 metaphases was counted (IPS cells used were at passage 10–15) and scored, up to 50 when mosaicism was suspected. Image acquisition was performed with an Axio Imager Z1 (ZEISS) and analyzed with IKAROS software (Metasystems).

3.4. Human genome CGH array

Genomic DNA extraction was performed as described above. Genome variation profiling by chromosomal microarray was conducted at ChromoStem® facility of Montpellier, France with a SurePrint G3 Human CGH Microarrays 8 × 60k (Agilent ®), and no additional CNV was detected in comparison to parental cells (Supplementary material 1 - RTS iPSC array CGH).

3.5. Detection of disease-causing mutations in RT gene

WRN mutations were confirmed by Sanger sequencing of PCR amplicons. Sanger sequencing was achieved using the BigDye® Terminator v1.1Cycle Sequencing Kit on the Applied Biosystems 3130xl. (Fig. 1, panel C).

3.6. Short tandem repeat analysis (STR)

Analysis was carried out at ChromoStem® facility of Montpellier, France, with a PowerPlex® 16 kit (Promega Corporation) and the GeneMarker V2.6.7 (SoftGenetics) on 13 STR (Supplementary material 2 - RTS iPSC STR analysis).

3.7. Flow cytometry analysis

BD Stemflow Human Pluripotent Stem Cell Transcription Factor Analysis Kit. Cells were analyzed on a CANTO II Becton Dickinson and analysis was made with Flow-JO. The results are presented in Fig. 1, panel B and antibodies used are in Table 1.

3.8. Immunofluorescence

Cells grown on coverslips were fixed in 4% paraformaldehyde in PBS and labeled overnight at room temperature, after 0,1% Saponin permeabilization in the blocking buffer (5% goat serum) for 60 min according to the standard protocol of StemLightTM Pluripotency Antibody Kit (Cell Signaling, no.9656). Antibodies panel, listed in Table 1, included: Oct-4A, Sox2, Nanog, SSEA4, TRA-1–60, TRA-1–81. Appropriate fluorochrome-conjugated anti primary antibodies with Alexa Fluor® 488 and Alexa Fluor® 555 dyes were applied 60 min. DNA was stained with DAPI (ImmunoChemistry, no.6244) 15 min and coverslips mounted in Vectashield (Vector, no.H-1400). Image acquisition was performed with an Axio Imager Z1(ZEISS) Apotome, X10 objective (Table 2).

3.9. Transcriptomic analysis

Total RNA isolation was performed using the RNeasy mini kit (Qiagen) according to the manufacturer's instructions. RNA was hybridized on an Affymetrix GeneChip Human Genome U133 Plus 2.0 array (shown in Fig. 1, panel E) at the transcriptomic facility IRMB/CHU, Montpellier, France (https://www.polebiosante-rabelais.fr/index.php/plateformes/autres-plateformes/276-center-hospitalier-universitaire-de-montpellier).

3.10. Teratoma formation

The differentiation potency was performed by in vivo teratoma derivation. Clusters corresponding to approximately 3 × 10^6 iPSC cells were injected into anesthetized NOD SCID gamma (NOD.CgPrkdcscidIl2rg tm1Wjl/SzJ). Mice were transplanted subcutaneously in the dorsolateral area on both sides at 8weeks old. After 4–8 weeks of latency, a 100% derivation efficiency was observed and teratomas were fixed, embedded in paraffin blocks, stained with Hematoxylin-Eosin-Saffron and analyzed by a pathologist for the presence of structures corresponding to the 3 embryonic germ layers (shown in Fig. 1, panel F).

3.11. Mitochondrial membrane potential

Membrane potential was measured with JC-1 dye (MitoProbe™ JC-1 Assay Kit, Thermo Fisher Scientific). JC-1 dye exhibits potential-dependent accumulation in mitochondria, indicated by a fluorescence emission shift from green (529 nm) to red (590 nm) after a 30 min incubation at 37 °C. In these conditions, the red/green fluorescence intensity ratio is representative of the mitochondrial membrane potential. Negative controls were made by adding a mitochondrial membrane-potential disrupter (CCCP) to aliquots of cells and staining with JC-1 in the same conditions, following the supplier instructions. Fluorescent intensity was measured by flow cytometry.

Declaration of Competing Interest

None.

Acknowledgments

The Montpellier public hospital Ingestem SAFE-iPS® and the ChromoStem® platforms are thanked for their support during this work. This work has been partially funded by the Montpellier public hospital centerthrough the “AOI Jeunes Chercheurs 2013” program.

Supplementary materials

Supplementary material associated with this article can be found, in

the online version, at doi:10.1016/j.scr.2020.101807.

References

Gatinois, V., Desprat, R., Becker, F., Pichard, L., Bernex, F., Corsini, C., Pellestor, F., Lemaitre, J.-.M., 2019a. Reprogramming of Human Peripheral Blood Mononuclear Cell (PBMC) from a patient suffering of a Werner syndrome resulting in iPSC line (REGUi003-A) maintaining a short telomere length. Stem Cell Res. 39, 101515. https://doi.org/10.1016/j.scr.2019.101515.

Gatinois, V., Desprat, R., Becker, F., Pichard, L., Bernex, F., Isidor, B., Pellestor, F., Lemaitre, J.-M., 2019b. iPSC line derived from a bloom syndrome patient retains an increased disease-specific sister-chromatid exchange activity. Stem Cell Res. 43, 101696. https://doi.org/10.1016/j.scr.2019.101696.

Guenther, M.G., Frampton, G.M., Soldner, F., Hockemeyer, D., Mitalipova, M., Jaenisch, R., Young, R.A., 2010. Chromatin structure and gene expression programs of human embryonic and induced pluripotent stem cells. Cell Stem Cell 7, 249–257. https://doi.org/10.1016/j.stem.2010.06.015.

Lapasset, L., Milhavet, O., Prieur, A., Besnard, E., Babled, A., Aït-Hamou, N., Leschik, J., Pellestor, F., Ramirez, J.-.M., De Vos, J., Lehmann, S., Lemaitre, J.-.M., 2011. Rejuvenating senescent and centenarian human cells by reprogramming through the pluripotent state. Genes Dev 25, 2248–2253. https://doi.org/10.1101/gad.173922.111.

Lu, L., Jin, W., Wang, L.L., 2017. Aging in Rothmund-Thomson syndrome and related RECQL4 genetic disorders. Ageing Res. Rev. 33, 30–35. https://doi.org/10.1016/j.arr.2016.06.002.